



Intrinsic activity of interfacial sites for Pt-Fe and Pt-Mo catalysts in the hydrogenation of carbonyl groups

Inssoo Ro^{a,1}, Isaias B. Aragao^{a,b}, Zachary J. Brentzel^a, Yifei Liu^a, Keishla R. Rivera-Dones^a, Madelyn R. Ball^a, Daniela Zanchet^b, George W. Huber^{a,*}, James A. Dumesic^{a,*}

^a Department of Chemical and Biological Engineering, University of Wisconsin-Madison, 1415 Engineering Drive, Madison, WI, 53706, United States

^b Institute of Chemistry, University of Campinas (UNICAMP), P.O. Box 6154, 13083-970, Campinas, São Paulo, Brazil



ARTICLE INFO

Keywords:
 Interfacial sites
 Bimetallic catalyst
 Active site
 Controlled surface reactions (CSR)
 Ketone hydrogenation
 Aldehyde hydrogenation

ABSTRACT

Bimetallic PtFe/SiO₂ and PtMo/SiO₂ catalysts were prepared using controlled surface reactions (CSR) of (cyclohexadiene)iron tricarbonyl and (cycloheptatriene)molybdenum tricarbonyl on a Pt/SiO₂ parent material. These catalysts were studied for the hydrogenation of ketone and aldehyde groups. Selective deposition of Fe onto Pt nanoparticles via the CSR method was confirmed by UV-vis absorption spectroscopy, scanning transmission electron microscopy, and inductively coupled plasma absorption emission spectroscopy. The oxidation states of the Pt and Fe species for PtFe catalysts were determined following treatment in H₂ at 573 K using X-ray photoelectron spectroscopy, showing that the dominant Pt phase is metallic Pt, while Fe is present in the metallic and +2 oxidation states, and Mo is present as a mixture of metallic, +4, and +6 oxidation states. The turnover frequency (TOF) of a Pt site for acetone (ketone) hydrogenation at 353 K and atmospheric pressure is 0.9 min⁻¹, whereas the TOF values of Pt-Fe_xO_y and Pt-MoO_x sites are 93 and 76 min⁻¹, respectively. For the hydrogenation of 2-hydroxytetrahydropyran (2-HY-THP, aldehyde) at 393 K and 30 bar pressure, the TOF of a Pt site is 7.8 min⁻¹, while the TOF values of Pt-Fe_xO_y and Pt-MoO_x sites are 480 and 830 min⁻¹, respectively. The order of magnitude enhancement of the TOF on the Pt-Fe_xO_y and Pt-MoO_x interfacial sites compared to that of the Pt site suggests that the Pt-metal oxide interface created on Pt catalysts by selective addition of Fe and Mo are active sites for both acetone and 2-HY-THP hydrogenation reactions. The presence of interfacial sites may enhance the catalytic activity over PtFe/SiO₂ and PtMo/SiO₂ catalysts by stabilization of adsorbed reactive intermediates through bonding with C=O groups.

1. Introduction

Supported Pt catalysts have been widely studied for the catalytic hydrogenation of various unsaturated bonds, including C=C, C≡C, and C=O moieties [1–4]. It has been demonstrated that incorporation of oxophilic metals onto Pt nanoparticles enhances the catalytic activity for hydrogenation reactions [5–8]. Somorjai et al. found that the addition of Fe to Pt nanoparticle catalysts increased the catalytic hydrogenation of ethylene and cyclohexene [5]. Ponec et al. reported that addition of Fe, Ga, and Ge enhanced the activity of supported Pt catalysts for the hydrogenation of acetone and propanal [3]. In addition, the incorporation of promoting materials (e.g. Sn, Fe, Co, and Ni) onto Pt catalysts has been reported to achieve selective hydrogenation of C=O versus C=C bonds [7,9].

The promotional effects of metallic additives, such as electronic (ligand) effects [7,10,11], lattice strain effects [10], geometric

(ensemble) effects [12], and surface adsorption of inactive species [5], have been studied to explain the improved performance of Pt catalysts. It has been suggested that addition of Fe to Pt weakens the adsorption of inactive spectator species on the catalyst surface for the hydrogenation of ethylene and cyclohexene [5]. The addition of Fe to Pt was also reported to induce electron transfer from more electropositive Fe to Pt. It has been reported that electron-deficient Fe behaves as a Lewis adsorption site for interaction with the oxygen of the C=O bond, where the polarized functional group is hydrogenated with hydrogen atoms adsorbed on nearby Pt atoms [7,13]. Density functional theory (DFT) calculations have shown that sub-surface 3d transition metal atoms can modify the electronic and chemical properties of a Pt surface by ligand effects or by the combination of strain and ligand effects [10,11]. The change in the energy of the surface d-band by the interactions with the subsurface 3d metal causes a change in the dissociative adsorption energy and adsorption properties of molecules [10,11].

* Corresponding authors.

E-mail addresses: gwhuber@wisc.edu (G.W. Huber), jdumesic@wisc.edu (J.A. Dumesic).

¹ Current address: Department of Chemical Engineering, University of California, Santa Barbara, CA 93106, United States.

It has been reported that tetrahydrofurfuryl alcohol (THFA) can be converted into 1,5-pentanediol (1,5-PD) in high yields using a reaction pathway in which THFA is initially converted into dihydropyran (DHP) over a solid acid catalyst, γ -Al₂O₃ [14]. The DHP is then hydrated to 2-hydroxytetrahydropyran (2-HY-THP), and 2-HY-THP is then hydrogenated into 1,5-PD over supported Ru catalysts. The key step in this pathway is hydrogenation of the ring-opened tautomer, 5-hydroxyvaleraldehyde (5-HY-Val), into 1,5-PD.

The objective of this work is to elucidate the catalytically active sites and measure the intrinsic catalytic activity for hydrogenation of a carbonyl group on interfacial sites. In this work, we have employed a synthetic method to prepare Pt/SiO₂ catalysts containing different amounts of Fe and Mo using controlled surface reactions (CSR). This method allows for the synthesis of controlled concentrations of Pt-Fe_xO_y and Pt-MoO_x interfacial sites that have well defined particle sizes. We have previously used this technique to measure the intrinsic activity of Pt-MoO_x, Cu-ZrO₂, and Au-MoO_x interfacial sites for ethanol conversion to ethyl acetate, methanol synthesis, and reverse water gas shift reactions [15–18]. Acetone and 2-HY-THP hydrogenation were used as probe reactions to investigate the effects of forming Pt-metal oxide interfacial sites on the hydrogenation of carbonyl compounds over supported Pt catalysts. We quantified the concentrations of Pt and Pt-metal oxide interfacial sites using CO chemisorption and measured the catalytic activity of these sites.

2. Experimental

2.1. Catalyst preparation

Monometallic 5 wt% Pt/SiO₂ was prepared by an incipient wetness impregnation of SiO₂ (Davilis grade 646, Sigma-Aldrich) with an aqueous solution of chloroplatinic acid hexahydrate (H₂PtCl₆·6H₂O) (Sigma-Aldrich), as described in detail elsewhere [17]. The SiO₂ support was crushed and sieved to between 60 and 100 mesh (0.150–0.250 mm) and washed with 5% nitric acid (HNO₃, Sigma-Aldrich) for 24 h before the synthesis. The sample was dried at 383 K in air for 2 h, reduced under hydrogen flow at 573 K, and then passivated at room temperature with 1% O₂ in Ar. Bimetallic PtFe and PtMo catalysts were synthesized by the CSR method following the procedure described elsewhere [15–21]. The Pt reference catalyst was reduced in a Schlenk tube, sealed, and then transferred to a glove box for Fe or Mo deposition without air exposure. A solution of (cyclohexadiene)iron tricarbonyl (Strem Chemicals) or (cycloheptatriene)molybdenum tricarbonyl (Strem Chemicals) in *n*-pentane was added onto the reduced Pt reference catalyst in the Schlenk tube and stirred for 2 h for the synthesis of Pt₁Fe_x/SiO₂ and Pt₁Mo_x/SiO₂, respectively. The mixture was transferred to a Schlenk line for evaporation of solvent remaining in the Schlenk tube. The sample was then reduced under hydrogen flow for 2 h and passivated at room temperature with 1% O₂ in He. Hereafter, prepared bimetallic catalysts will be referred to as Pt₁Fe_x or Pt₁Mo_x, where x is equal to the nominal Fe (or Mo)/Pt atomic ratio.

A 0.5wt% Pt/H-ZSM-5 catalyst was prepared by an ion-exchange method described elsewhere [22]. The H-ZSM-5 (SiO₂:Al₂O₃ = 80, Z-80) support (Zeolyst) was calcined at 873 K for 18 h (with a heating rate of 1 K min⁻¹) before the synthesis. H-ZSM-5 (Z-80) was dispersed in Milli-Q water, and tetraammineplatinum(II) nitrate [[Pt(NH₃)₄](NO₃)₂, Sigma-Aldrich] solution was added into the suspension. The mixture was aged for 24 h under continuous mixing at room temperature and was then centrifuged to separate the solid. The separated solid was dispersed in a new aqueous solution containing tetraammine platinum (II) nitrate. The synthesis sequence was repeated three times. After the 3rd cycle, the solid recovered after centrifugation was filtered, washed with Milli-Q water, and dried at 383 K overnight. The sample was calcined at 573 K under air flow for 1 h.

2.2. Reactivity measurements

The catalytic activity for gas-phase acetone hydrogenation was evaluated in a fixed-bed quartz reactor at atmospheric pressure. Prior to reactivity measurements, catalysts were reduced in situ at 573 K (with a heating rate of 3 K min⁻¹) under H₂ flow (20 cm³ (STP) min⁻¹) for 2 h. Catalysts (1–100 mg) were diluted with 150–500 mg of crushed silica chips (silicon dioxide, fused, 60–100 mesh, Sigma Aldrich) and placed in the center of the reactor. Liquid acetone (> 99.5%, Fisher Scientific) was fed to the reactor system at a flow rate of 0.75 μ L/min at room temperature using a syringe pump (Harvard Apparatus) and vaporized at the reactor inlet by being mixed into He and H₂ flowing at rates of 25 and 5 cm³ (STP) min⁻¹, respectively. The temperature of the reactor was measured using a K-type thermocouple attached to the outside of the reactor wall. The reaction temperature was adjusted by a variable autotransformer power source connected to a tube furnace. Control experiments without catalyst confirmed the absence of reactivity from the reactor. Reaction products were analyzed by an online gas chromatograph with a barrier discharge ionization detector (GC-BID) system (Shimadzu). The acetone hydrogenation reaction rate was measured at 353 K after 1 h, and the turnover frequency (TOF) was calculated using the number of Pt sites measured by CO chemisorption. Internal mass transport limitations were predicted to be negligible for our catalysts in the acetone hydrogenation reaction according to the Thiele modulus calculation. Details of the calculation for the Thiele modulus and the effectiveness factor are listed in Table S1.

The liquid-phase hydrogenation of 2-HY-THP was performed in both batch and fixed bed catalytic reactors. Batch reactions were carried out in 45 mL Hastelloy high-pressure batch reactors (PARR series 5000 Multi Reactor System equipped with 4871 Process Controller). First, the catalyst and magnetic stir bar were loaded into the reactor. The reactor was purged with 20 bar of He three times and purged again with 20 bar of H₂ three times, followed by pressurizing to 20 bar of H₂. Then, catalysts were reduced in situ at 473 K (with a heating rate of 2 K min⁻¹) under 20 bar of H₂. 20 mL of a feed solution containing 10 wt% of 2-HY-THP (Acros Organics, 90%) in Milli-Q water was introduced into the vessels and mixed with catalyst using a magnetic stir bar (550 rpm). The vessel was sealed and pressurized with 30 bar of H₂, and then heated to 393 K for 15 min and held for 60 min. All experiments were performed at conversions lower than 35% of the equilibrium conversion.

The stability of catalysts for the liquid-phase hydrogenation of 2-HY-THP reaction was studied in an up-flow, fixed-bed quarter-inch stainless steel reactor at 30 bar and 393 K with Pt₁Fe_{0.2}/SiO₂. The reactor void space was filled with fused SiO₂ chips (Sigma, 99.9%, 4–20 mesh) to decrease void volume and increase heat transfer. The catalyst was placed between two plugs of quartz wool (Ohio Valley Specialty Chemicals) in the center of the reactor. The tube was secured with aluminum blocks in a 1450 W furnace (Applied Test Systems, Inc.). Liquid phase solution containing 10 wt% 2-HY-THP was fed into the reactor system at a flow rate of 2 mL/min at room temperature using a high-performance liquid chromatography (HPLC) pump (Lab Alliance Series) with H₂ flowing at the rate of 30 cm³ (STP) min⁻¹. Liquid reaction products obtained from 2-HY-THP hydrogenation were collected from the condensed effluent every 2–24 h. Liquid reaction products from both batch and continuous flow reactors were filtered using a 0.2 μ m PTFE (polytetrafluoroethylene) syringe filter and analyzed by HPLC (Waters Alliance 2695 system equipped with a Waters 410 differential refractometer) with an Aminex HPX-87H ion exchange column and 5 mM H₂SO₄ mobile phase.

2.3. Catalyst characterization

2.3.1. Fourier transform infrared spectroscopy (FT-IR)

Catalyst samples were pressed into self-supporting pellets with a 0.9–1.1 cm die. Pt/SiO₂ and Pt₁Fe_x/SiO₂ pellets were mounted in the

Table 1Characterization of Pt/SiO₂, Pt₁Fe_x/SiO₂, and Pt₁Mo_x/SiO₂ catalysts.

Sample	Pt wt% (ICP)	Fe (or Mo) wt% (ICP)	Fe (or Mo)/Pt molar ratio (Nominal)	Fe (or Mo)/Pt molar ratio (ICP)	Fe (or Mo)/Pt molar ratio (EDS)	CO uptake (μmol g ⁻¹)	Reference
Pt/SiO ₂	4.9	0	0	0	0	38.0	Current work
Pt ₁ Fe _{0.025} /SiO ₂	4.7	0.04	0.025	0.03	0.03	30.7	Current work
Pt ₁ Fe _{0.05} /SiO ₂	4.7	0.07	0.05	0.06	0.04	27.9	Current work
Pt ₁ Fe _{0.1} /SiO ₂	4.7	0.09	0.1	0.08	0.06	25.3	Current work
Pt ₁ Fe _{0.2} /SiO ₂	4.6	0.21	0.2	0.16	0.04	20.8	Current work
Pt ₁ Mo _{0.15} /SiO ₂	4.7	0.26	0.15	0.11	0.09	20.7	[17]
Pt ₁ Mo _{0.3} /SiO ₂	4.4	0.52	0.3	0.24	0.13	15.2	[17]
Pt ₁ Mo _{0.45} /SiO ₂	4.3	0.85	0.45	0.40	0.15	8.5	[17]

sample holder of a transmission cell described elsewhere [15,18,23,24] and reduced in flowing H₂ at 573 K. After reduction, the sample was cooled under H₂ flow to room temperature and evacuated to 10⁻⁵ Torr, and a background scan was then recorded. Fourier transform infrared (FTIR) (Nicolet 6700) spectra of adsorbed CO were obtained in transmission mode after dosing 800 Torr of 1% CO in He (Airgas), holding for 10 min, and evacuating under He flow for 10 min. The temperature was measured by a K-type thermocouple and heating was controlled by a PID controller. The sample holder was designed for collecting spectra at temperatures from 150 to 600 K, as described previously [15,18,23,24]. All spectra were collected by averaging 256 scans with a resolution of 4 cm⁻¹. Spectral deconvolution was performed using Origin 9.1 to determine the areal contribution from each peak. The final spectrum of CO adsorbed on each catalyst was represented by two superimposed Gaussian curves, as described elsewhere [18].

2.3.2. CO chemisorption

The CO chemisorption studies were carried out using a Micromeritics ASAP 2020C system. The catalysts were reduced under H₂ flow at 573 K, and CO adsorption was performed at 308 K after reduction. The adsorption stoichiometry between CO and surface Pt sites was assumed to be 1:1, as reported previously [17]. CO chemisorption was used to estimate the number of Pt metallic and Pt-Fe_xO_y interfacial sites. The number of Pt-Fe_xO_y interfacial sites was determined from the decrease in the number of Pt sites upon addition of Fe, with the assumption that the deposition of Fe occurs on Pt sites with 1:1 stoichiometry, as reported previously [15–19].

2.3.3. Inductively coupled plasma-absorption emission spectroscopy (ICP-AES)

The Pt and Fe loadings of catalysts were determined using a Perkin-Elmer Plasma 400 ICP Emission Spectrometer. Typically, 50 mg of catalyst samples were digested with a mixture of 2 mL of nitric acid (Fischer, 65 wt%) and 6 mL of hydrochloric acid (Fischer, 37 wt%) by refluxing at 423 K for 14 h. Pt and Fe standards for the ICP analysis were prepared from Pt and Fe ICP standards (Fluka, 1000 ± 2 mg L⁻¹). The post-digestion mixture was cooled to room temperature, diluted in water, filtered, and analyzed with the ICP emission spectrometer.

2.3.4. Ultraviolet-visible (UV-vis) absorption spectroscopy

UV-vis absorption spectra over the wavelength range 200–600 nm were recorded using a Thermo Scientific Evolution 300 UV-vis spectrometer with 1 cm path-length quartz cuvette. The Fe concentration was calibrated at the wavelength of 280 nm to measure the percentage of Fe precursor deposition onto the reference Pt/SiO₂ catalyst.

2.3.5. Scanning transmission electron microscopy/energy-dispersive X-ray spectroscopy (STEM/EDS)

A FEI Titan STEM with Cs probe aberration corrector operated at 200 kV with spatial resolution < 0.1 nm was used for scanning transmission electron microscopy (STEM) studies. Images were collected

using high-angle annular dark-field (HAADF) mode, with HAADF detector angle ranging from 54 to 270 mrad, probe convergence angle of 24.5 mrad, and probe current of approximately 25 pA. Energy dispersive x-ray spectroscopy (EDS) data were collected using the same microscope with an EDAX SiLi Detector. Catalyst samples were suspended in ethanol and then dropped on a holey carbon Cu TEM grid. Samples were plasma cleaned before being loaded into the microscope.

2.3.6. X-ray photoelectron spectroscopy (XPS)

A Thermo Scientific K-Alpha system equipped with a monochromatic Al K α as X-ray source was used for XPS characterization. XPS spectra were obtained with samples which were reduced in H₂ at 573 K and transferred into the XPS without air exposure using Transfer Vessel K-Alpha (Thermo Scientific). Surface charging effects derived from monochromatic X-rays were suppressed by the usage of a flood gun which neutralizes surface charging. The binding energies were calibrated based on the C1s peak at 284.8 eV as a reference.

3. Results and discussion

Table 1 shows characterization results for Pt/SiO₂, Pt₁Fe_x/SiO₂, and Pt₁Mo_x/SiO₂ catalysts. The loadings of Pt, Fe, and Mo of prepared catalysts were determined by ICP and EDS measurements. The actual Fe/Pt molar ratios of Pt₁Fe_x/SiO₂ samples determined by ICP and EDS analysis are close to the nominal molar ratios up to a Fe/Pt molar ratio of 0.05. The Fe/Pt molar ratio estimated by EDS is lower than the measurement from ICP, with the discrepancy increasing as the Fe loading increases, as previously reported with Pt₁Mo_x/SiO₂ catalysts [17]. As shown in **Fig. 1**, the Fe/Pt molar ratio of Pt₁Fe_{0.05}/SiO₂ estimated by STEM-EDS is 0.04, in agreement with the nominal and actual loadings measured by ICP. This result suggests that the Fe precursor has been uniformly deposited only onto Pt nanoparticles with the CSR method up to a Fe/Pt molar ratio of 0.05. We have previously demonstrated that the Pt particle size and morphology do not change after deposition of the promoting material(s) using the CSR method [17,25]. Selective deposition of Fe precursor onto Pt sites during synthesis of Pt₁Fe_{0.05}/SiO₂ by CSR was further evidenced by UV-vis absorption spectroscopy, as reported in detail elsewhere [26]. For example, as presented in **Fig. 2**, the spectra of the Fe precursor in the *n*-pentane solution before and after contact with the reference Pt/SiO₂ catalyst indicate that approximately 95% of Fe precursor was deposited onto Pt catalysts. In contrast, no difference was observed in the spectra of the Fe precursor in the *n*-pentane solution before and after contact with SiO₂. These characterization results suggest selective deposition of Fe on Pt sites up to a Fe/Pt molar ratio of 0.05. There was no further deposition of Fe above a Fe/Pt molar ratio of 0.2 on the 5 wt% Pt/SiO₂ catalyst. In addition, deposition of Fe to a molar ratio of 0.2 by changing the loading of Pt was not successful. This result suggests that Pt sites become saturated above the Fe loading of 0.2. CO chemisorption was used to measure the number of metallic Pt sites of Pt/SiO₂, Pt₁Fe_x/SiO₂, and Pt₁Mo_x/SiO₂. The CO uptake decreases with increasing Fe loading of the Pt₁Fe_x/SiO₂ catalysts prepared by the CSR method,

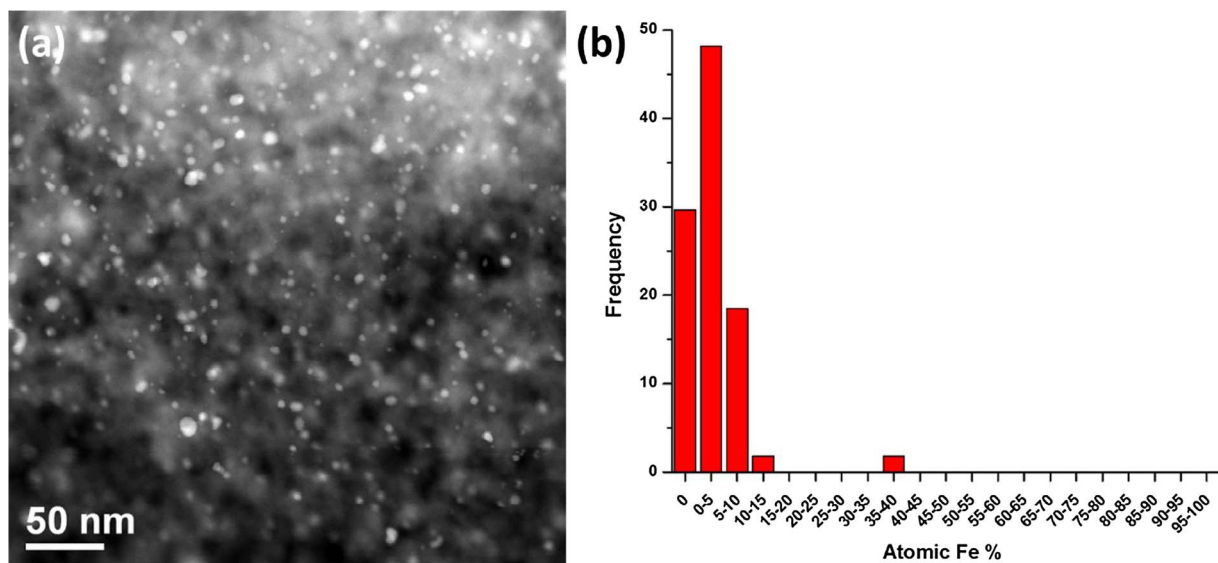


Fig. 1. (a) STEM image and (b) EDS histogram of Fe content for the $\text{Pt}_1\text{Fe}_{0.05}/\text{SiO}_2$ catalyst. The particle size distribution for this catalyst can be found in Fig. S1 of the supplemental information.

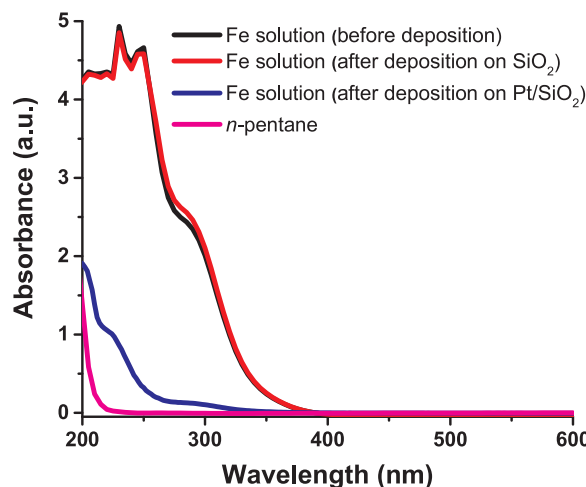


Fig. 2. UV-vis absorption spectra of Fe precursor solution in *n*-pentane before (black) after deposition onto the SiO_2 support (red) and reference Pt/SiO_2 (blue). (For interpretation of the references to colour in this figure legend, the reader is referred to the web version of this article).

suggesting that Fe has been selectively deposited on Pt sites. The $\text{Pt}_1\text{Mo}_{0.2}/\text{SiO}_2$ catalysts showed a similar decreasing trend of the CO uptake as the Mo loading increased, as reported previously [17].

Fig. 3 shows the XPS spectrum of Pt (4f_{5/2} and 4f_{7/2}) and Fe (2p_{3/2} and 2p_{1/2}) for the $\text{Pt}_1\text{Fe}_{0.2}/\text{SiO}_2$ catalyst after *in situ* reduction in H_2 at 573 K. As shown in Fig. 3(a), the Pt 4f doublet peaks are observed at 71.5 and 74.8 eV, corresponding to Pt 4f_{7/2} and 4f_{5/2} binding energy in oxidation state of Pt° , as reported previously [27–29]. This result indicates the dominance of Pt° species in the $\text{Pt}_1\text{Fe}_{0.2}/\text{SiO}_2$ catalyst, in agreement with previous studies of supported Pt nanoparticles catalysts after reduction [30]. Fig. 3(b) shows the XPS signal for Fe in $\text{Pt}_1\text{Fe}_{0.2}/\text{SiO}_2$ catalyst. According to previous studies, the Fe 2p_{3/2} main peaks found at 706.9, 709.7, and 713.1 eV can be assigned to Fe° , Fe^{2+} , and Fe^{3+} states [31–33]. This result suggests the coexistence of both metallic iron and iron oxide after reduction. According to the X-ray absorption near edge structure (XANES) characterization result of $\text{Pt}_1\text{Fe}_{0.2}/\text{SiO}_2$, the dominant oxidation state of Fe is a combination of Fe° and Fe^{2+} [19].

Fig. 4 shows infrared spectra of CO chemisorbed on the reference Pt/SiO_2 and the $\text{Pt}_1\text{Fe}_{0.2}/\text{SiO}_2$ catalysts, collected at 298 K after *in-situ*

reduction in flowing H_2 at 573 K. The total peak area of the $\text{Pt}_1\text{Fe}_{0.2}/\text{SiO}_2$ catalysts (CSR) is lower than the reference Pt/SiO_2 , further demonstrating that Fe species were deposited on Pt sites by the CSR method. This result is in agreement with the trends observed from the EDS and CO chemisorption, as shown in Table 1. The spectra of the reference Pt/SiO_2 and the $\text{Pt}_1\text{Fe}_{0.2}/\text{SiO}_2$ catalysts are asymmetrical and can be deconvoluted into two peaks, corresponding to a peak near 2078 cm⁻¹ and a shoulder peak near 2048 cm⁻¹. The two bands at 2075–2082 and 2040–2050 cm⁻¹ are in agreement with results of previous studies of supported Pt catalysts ([34–38] : ACS Catal. 6, 8, 5599–5609). Arai and co-workers ascribed a band at 2080 cm⁻¹ and a shoulder band at 2040 cm⁻¹ to CO adsorbed on Pt terrace sites and on Pt edge, corner and/or kink sites, respectively [34,35]. Bocuzzi and Greenler suggested that the lower frequency band can be associated to CO adsorbed on under-coordinated (defect) sites and the high frequency band to terrace sites [36–38]. They ascribed two bands at 2077 and 2057 cm⁻¹ to terrace and kink sites, respectively [36–38]. The band at 2070–2090 cm⁻¹ was also assigned to CO linearly adsorbed on fully reduced Pt (Pt°) sites in other studies, in agreement with XPS characterization shown in Fig. 3 [39–41]. In single-crystal studies, Xu and Yates assigned bands at 2070 cm⁻¹ and 2064 cm⁻¹ to CO linearly-adsorbed on a Pt (335) and Pt (112) surfaces, respectively [42]. Spectral deconvolution was performed to obtain the spectral areas of the CO bands at 2077 and 2048 cm⁻¹ for the $\text{Pt}_1\text{Fe}_{0.2}/\text{SiO}_2$ catalysts. The constant shape of the bands before and after Fe deposition suggests the uniform deposition of Fe on both under- and highly-coordinated Pt sites by CSR.

3.1. Catalytic activity measurements

Table 2 shows the rate and TOF for acetone hydrogenation over the Pt/SiO_2 and $\text{Pt}_1\text{Fe}_{0.2}/\text{SiO}_2$ catalysts. All catalysts showed 100% selectivity to isopropanol (IPA) under these reaction conditions. The rate and TOF of acetone hydrogenation over Pt/SiO_2 catalyst is in agreement with the rate and TOF measured at 303 K reported by Vannice and Sen [43]. The reported TOF at the reaction temperature of 303 K is 0.4–0.8 min⁻¹ [43]. The overall reaction rate and TOF of acetone (ketone) hydrogenation over the $\text{Pt}_1\text{Fe}_{0.2}/\text{SiO}_2$ increased by an order of magnitude compared to the reaction rate and TOF over Pt/SiO_2 catalyst. Selective deposition of a trace amount of Fe (a Fe/Pt atomic ratio of 0.05) on Pt by CSR increased the reaction rate by a factor of 30, indicating the importance of $\text{Pt}-\text{Fe}_{0.2}\text{O}_y$ interfacial sites in catalytic

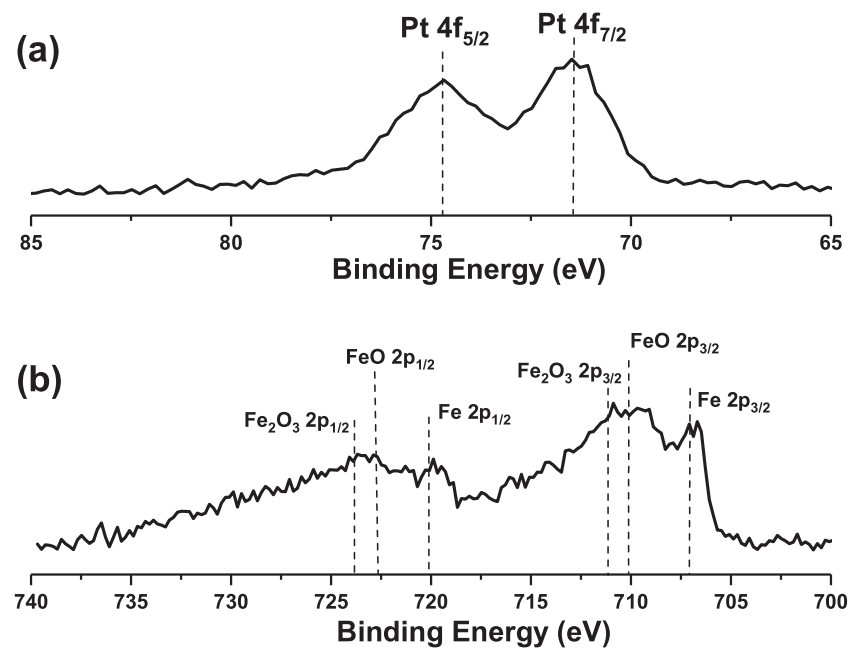


Fig. 3. XPS spectra of $\text{Pt}_1\text{Fe}_{0.2}/\text{SiO}_2$ catalyst after in situ reduction at 573 K. XPS spectrum of (a) $\text{Pt } 4\text{f}_{7/2}$ and $4\text{f}_{5/2}$ and (b) $\text{Fe } 2\text{p}_{3/2}$ and $\text{Fe } 2\text{p}_{1/2}$.

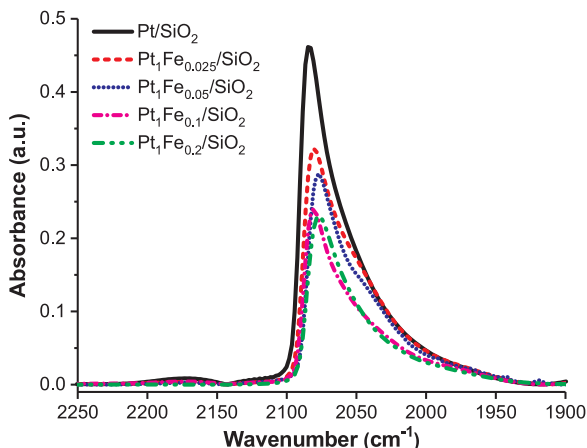


Fig. 4. IR spectra collected at 298 K of in situ reduced Pt/SiO_2 and $\text{Pt}_1\text{Fe}_x/\text{SiO}_2$ catalysts after introduction of 8 Torr CO, and followed by 10 min evacuation under He flow. Intensities are normalized by pellet density. IR spectra of in situ reduced $\text{Pt}_1\text{Mo}_x/\text{SiO}_2$ catalysts can be found in Fig. S2 of the supplemental information.

Table 2
Experimentally measured reaction rate and TOF for acetone hydrogenation.^a

Sample	Acetone Conversion Rate ($\mu\text{mol g}_{\text{cat}}^{-1} \text{min}^{-1}$)	TOF (min ⁻¹)
Pt/SiO_2	35	1
$\text{Pt}_1\text{Fe}_{0.025}/\text{SiO}_2$	170	5
$\text{Pt}_1\text{Fe}_{0.05}/\text{SiO}_2$	1140	41
$\text{Pt}_1\text{Fe}_{0.1}/\text{SiO}_2$	1380	54
$\text{Pt}_1\text{Fe}_{0.2}/\text{SiO}_2$	1450	70
$\text{Pt}/\text{SiO}_2 + \text{Fe}_{0.2}/\text{SiO}_2$ ^b	40	1

^a Reaction temperature of 353 K and atmospheric pressure.

^b A physical mixture of two catalysts refers to Pt/SiO_2 mixed with $\text{Fe}_{0.2}/\text{SiO}_2$, and the conversion rate and TOF was calculated with the amount and the number of sites of Pt/SiO_2 , respectively.

activity for acetone hydrogenation reaction. The reaction rates and TOF of acetone hydrogenation increased with Fe loading to a Fe/Pt atomic ratio of 0.05 and became constant above this Fe loading. As seen in

Table 2, the TOF of a physical mixture is similar to that of Pt/SiO_2 , indicating that an intimate contact between Pt and Fe_xO_y is important for acetone hydrogenation reaction.

The catalytic activities of the Pt/SiO_2 and $\text{Pt}_1\text{Fe}_x/\text{SiO}_2$ catalysts were measured for the hydrogenation of 2-HY-THP, which is equilibrated with its ring-opened tautomer 5-hydroxyvaleraldehyde (5-HY-Val), into 1,5-PD. All catalysts showed nearly 100% selectivity to 1,5-PD under these reaction conditions. As seen in Table 3, the conversion rate and TOF of $\text{Pt}_1\text{Fe}_x/\text{SiO}_2$ catalysts are more than one order of magnitude higher than those of the Pt/SiO_2 catalyst for 2-HY-THP (aldehyde) hydrogenation. The enhanced activity for $\text{Pt}_1\text{Fe}_x/\text{SiO}_2$ catalysts compared to Pt/SiO_2 for acetone and 2-HY-THP hydrogenation reactions suggests that the formation of Pt-Fe interfacial site enhances catalytic activity of both ketone and aldehyde groups. The same low concentration of Pt-Fe interfacial sites (a Fe/Pt atomic ratio of 0.025) yields a higher promoting effect in 2-HY-THP reaction compared to acetone hydrogenation reaction. The rate of promotion of the Fe is greater for hydrogenation of an aldehyde than a ketone, in agreement with a previous report by Ponec et al. [3]. In addition, a physical mixture of Pt/SiO_2 and $\text{Fe}_{0.2}/\text{SiO}_2$ exhibited similar activity to Pt/SiO_2 , indicating that an intimate contact between Pt and Fe_xO_y is required for aldehyde hydrogenation.

$\text{Pt}_1\text{Mo}_x/\text{SiO}_2$ catalysts were also studied for the hydrogenation of acetone and 2-HY-THP. As seen in Table 4, hydrogenation rates for the

Table 3
Experimentally measured reaction rate and TOF for liquid phase 2-HY-THP hydrogenation.^a

Sample	2-HY-THP Conversion Rate ($\text{mmol g}_{\text{cat}}^{-1} \text{min}^{-1}$)	TOF (min ⁻¹)
Pt/SiO_2	0.3	8
$\text{Pt}_1\text{Fe}_{0.025}/\text{SiO}_2$	3.5	114
$\text{Pt}_1\text{Fe}_{0.05}/\text{SiO}_2$	3.5	125
$\text{Pt}_1\text{Fe}_{0.1}/\text{SiO}_2$	10	404
$\text{Pt}_1\text{Fe}_{0.2}/\text{SiO}_2$	8.5	406
$\text{Pt}/\text{SiO}_2 + \text{Fe}_{0.2}/\text{SiO}_2$ ^b	0.3	8

^a Reaction temperature of 393 K and pressure of 30 bar.

^b A physical mixture of two catalysts refers to Pt/SiO_2 mixed with $\text{Fe}_{0.2}/\text{SiO}_2$, and the conversion rate and TOF was calculated with the amount and the number of sites of Pt/SiO_2 , respectively.

Table 4

Experimentally measured reaction rate and TOF for acetone^a and 2-HY-THP^b hydrogenation over Pt/SiO₂ and Pt₁Mo_x/SiO₂ catalysts.

Sample	Acetone Conversion Rate ($\mu\text{mol g}_{\text{cat}}^{-1} \text{min}^{-1}$)	TOF for Acetone Conversion (min^{-1})	2-HY-THP Conversion Rate ($\text{mmol g}_{\text{cat}}^{-1} \text{min}^{-1}$)	TOF for 2-HY-THP Conversion (min^{-1})
Pt/SiO ₂	35	1	0.3	8
Pt ₁ Mo _{0.15} /SiO ₂	1580	76	29	1379
Pt ₁ Mo _{0.3} /SiO ₂	1760	116	14	948
Pt ₁ Mo _{0.45} /SiO ₂	1820	214	23	2737
Pt/SiO ₂ + Mo _{0.3} /SiO ₂ ^c	71	2	0.7	19

^a Reaction temperature of 353 K and atmospheric pressure.^b Reaction temperature of 393 K and pressure of 30 bar.^c A physical mixture of two catalysts refers to Pt/SiO₂ mixed with Mo_{0.3}/SiO₂, and the conversion rate and TOF was calculated with the amount and the number of sites of Pt/SiO₂, respectively.

Pt₁Mo_x/SiO₂ catalysts were more than two orders of magnitude higher than the rates of the Pt/SiO₂ catalyst for both reactions. The TOF of Pt₁Mo_{0.15}/SiO₂ for acetone hydrogenation is similar to that of PtFe/SiO₂ with a comparable Fe loading (Pt₁Fe_{0.2}/SiO₂). On the other hand, the TOF of Pt₁Mo_{0.15}/SiO₂ is three-fold higher than Pt₁Fe_{0.2}/SiO₂ in the 2-HY-THP hydrogenation reaction, suggesting that Pt-Mo interfacial sites are more active than Pt-Fe interfacial sites in the conversion of 2-HY-THP to 1,5-PD. A physical mixture of Pt/SiO₂ and Mo_{0.3}/SiO₂ exhibited only two times enhancement in the rate of acetone and 2-HY-THP hydrogenation reactions. This result provides further evidence that Pt-Mo interfacial sites are active sites for both hydrogenation reactions.

The stabilities of Pt/SiO₂, Pt₁Fe_{0.2}/SiO₂, and Pt₁Mo_{0.15}/SiO₂ catalysts were studied for 2-HY-THP hydrogenation in a continuous flow reactor. Fig. 5 shows the conversion of 2-HY-THP over catalysts at 393 K as a function of time on stream. Previous work has shown that supported Ru catalysts exhibit deactivation for the conversion of 2-HY-THP in a continuous flow reactor [14]. For example, a Ru/TiO₂ catalyst undergoes deactivation with a first-order deactivation constant (k_d) of 0.0086 h⁻¹. Subsequent re-reduction at 573 K or calcination at 603 K followed by reduction at 573 K did not restore the activity of Ru/TiO₂ catalyst. A Ru/C catalyst exhibited better stability, with a first order deactivation constant (k_d) of 0.002 h⁻¹. As shown in Fig. 5, the Pt/SiO₂, Pt₁Fe_{0.2}/SiO₂, and Pt₁Mo_{0.15}/SiO₂ catalysts exhibited modest deactivation with a deactivation constant of 0.002 h⁻¹. Although the deactivation constant of Pt₁Fe_{0.2}/SiO₂ and Pt₁Mo_{0.15}/SiO₂ catalysts is similar with that of Ru/C catalyst, the TOF values of the Pt₁Fe_{0.2}/SiO₂ and Pt₁Mo_{0.15}/SiO₂ catalysts are approximately 9 and 30 times higher, respectively, than the Ru/C catalyst under the same reaction conditions.

The number of Pt metallic sites was measured by CO chemisorption. The number of Pt-metal oxide interfacial sites was estimated from the change in the number of Pt sites by assuming that deposition of metal-oxide on Pt sites occurs with a 1:1 stoichiometry, as reported previously

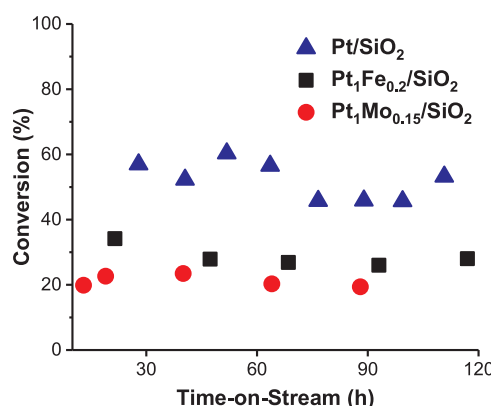


Fig. 5. Time-on-stream (TOS) behavior over 36 mg of Pt/SiO₂ (▲), 3.1 mg of Pt₁Fe_{0.2}/SiO₂ (■), 1.5 mg of Pt₁Mo_{0.15}/SiO₂ (●) catalysts at 393 K for 2-HY-THP hydrogenation reaction.

[15–19]. In addition, the number of Pt-metal oxide interfacial sites estimated by the actual Fe loading for comparison is included in Table S2. The discrepancy in number of Pt-Fe_xO_y interfacial sites estimated by CO chemisorption and by the Fe loading is negligible at low loadings, but it becomes larger at high loadings, as shown in Table S2. This result suggests that Fe species are selectively deposited on Pt sites at low loadings, but they start to aggregate at high loadings. The coordination number of Fe-Fe bonding for Pt₁Fe_{0.2}/SiO₂ after reduction is 1.7 and that of Fe-Pt is 3.6 according to the extended X-ray absorption fine structure (EXAFS) data we have previously reported [19]. These data suggest that Fe has more Fe-Pt bonds than Fe-Fe bonds, and Fe likely exists as highly dispersed moieties on the Pt/SiO₂ catalyst, suggesting the formation of Fe islands on the surface at high Fe loadings, in agreement with the results shown in Table S2.

The catalytic activities for the two different active sites (r_{Pt} and $r_{\text{Pt-metoxide}}$) were estimated using the number of Pt and Pt-metal oxide interfacial sites (S_{Pt} and $S_{\text{Pt-metoxide}}$) using Eq. (1).

$$R_{\text{total}} = R_{\text{Pt}} + R_{\text{Pt-metoxide}} = r_{\text{Pt}} S_{\text{Pt}} + r_{\text{Pt-metoxide}} S_{\text{Pt-metoxide}} \quad (1)$$

R_{Pt} and $R_{\text{Pt-metoxide}}$ refer to the moles of acetone converted into IPA per mass of catalyst per minute from monometallic Pt and Pt-metal oxide interfacial sites, whereas r_{Pt} and $r_{\text{Pt-metoxide}}$ indicate the turnover rates. S_{Pt} is the number of Pt sites per mass of catalyst, and $S_{\text{Pt-metoxide}}$ is the number of Pt-metal oxide interfacial sites site per mass. The experimental and model-predicted rates for acetone conversion to IPA over Pt/SiO₂, Pt₁Fe_x/SiO₂, and Pt₁Mo_x/SiO₂ catalysts are plotted in Fig. 6, using the following turnover rates: $r_{\text{Pt}} = 0.6 \text{ min}^{-1}$, $r_{\text{PtFe}_x\text{O}_y} = 93 \text{ min}^{-1}$, and $r_{\text{PtMo}_x} = 76 \text{ min}^{-1}$. This result suggests that the rates per Pt-Fe_xO_y site ($r_{\text{PtFe}_x\text{O}_y}$) and Pt-Mo_x site (r_{PtMo_x}) are approximately 100 and 80 times greater, respectively, than that of the Pt site (r_{Pt}) for acetone hydrogenation to IPA. The experimental and model-predicted rates for 2-HY-THP conversion to 1,5-PD are plotted in Fig. 7, using the following turnover rates: $r_{\text{Pt}} = 7.7 \text{ min}^{-1}$, $r_{\text{PtFe}_x\text{O}_y} = 480 \text{ min}^{-1}$, and $r_{\text{PtMo}_x} = 830 \text{ min}^{-1}$. This result suggests that the rates per Pt-Fe_xO_y site ($r_{\text{PtFe}_x\text{O}_y}$) and Pt-Mo_x site (r_{PtMo_x}) are approximately 60 and 100 times greater, respectively, than that of the Pt site (r_{Pt}) for 2-HY-THP hydrogenation to 1,5-PD.

The enhanced rates of carbonyl hydrogenation reactions over Pt₁Fe_x/SiO₂ and Pt₁Mo_x/SiO₂ catalysts may be ascribed to stabilization of the transition-states for the molecularly-adsorbed reactive intermediates by the presence of Pt-Fe and Pt-Mo interfacial sites. Previous work has suggested that promotion of hydrogenation can occur through (1) an increased electron density of Pt from the formation of metal alloys, (2) the formation of polar Pt-Fe (or Pt-Mo) interfacial sites that increases the interaction of the C=O bond with the catalyst surface [7,9], and/or (3) the creation of Lewis acid sites (Fe⁸⁺ and Mo⁸⁺) in close proximity to Pt by electron transfer from Fe to Pt which results in interactions with the lone electron pairs of the oxygen in C=O functional groups and subsequent activation of C=O bonds [7,9]. Hirshel et al. demonstrated using DFT calculations that a C=O bond can be weakened when Fe atoms are present on a Pt (111) surface compared to

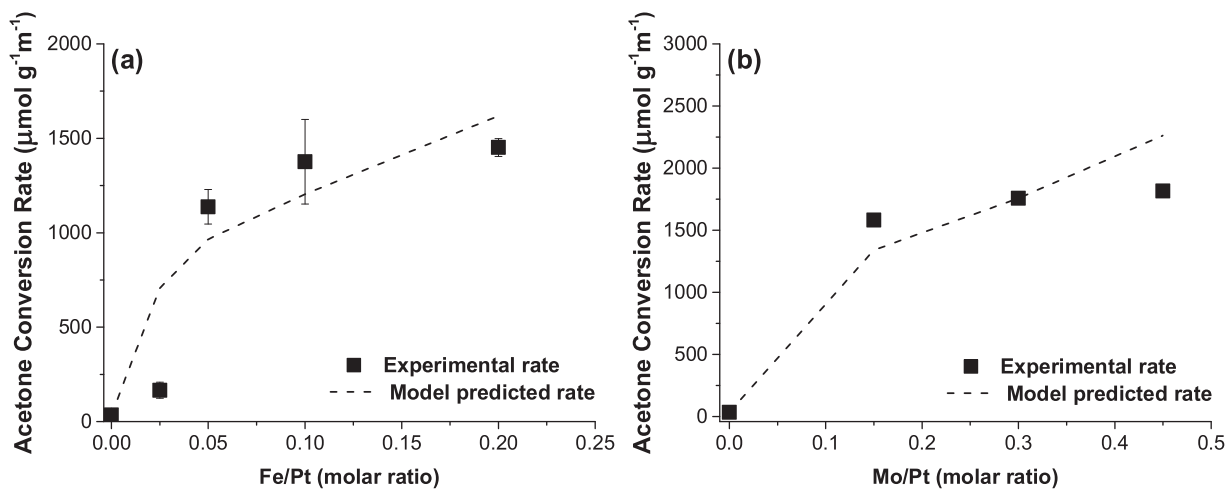


Fig. 6. Rate of acetone hydrogenation over (a) $\text{Pt}_1\text{Fe}_x/\text{SiO}_2$ and (b) $\text{Pt}_1\text{Mo}_x/\text{SiO}_2$ catalysts. The dashed line indicates model predicted rates. The model predictions are as follows: $r_{\text{Pt}} = 0.9 \text{ min}^{-1}$, $r_{\text{PtFe}_x\text{O}_y} = 93 \text{ min}^{-1}$, and $r_{\text{PtMo}_x} = 76 \text{ min}^{-1}$.

a pure Pt (111) surface from the strong interaction between Fe and O in $\text{C}=\text{O}$ bond [44]. In addition, it has been reported that the addition of promoting material (e.g. potassium) can increase the isobutane dehydrogenation reaction rate by stabilizing reactive intermediates on the surface of the supported Pt catalyst [45,46]. Reaction kinetics experiments for acetone hydrogenation showed that the acetone and H_2 reaction orders were both approximately 0.5 over the Pt/SiO_2 and $\text{Pt}_1\text{Fe}_{0.05}/\text{SiO}_2$ catalysts. Thus, it appears that the essential aspects of the reaction mechanism for acetone hydrogenation are the same for both catalysts.

A redox mechanism has been proposed to explain the enhanced activity for different reactions such as CO oxidation and water gas shift [47,48]. Tai and co-workers demonstrated that a change in the oxidation state of Fe between Fe^{2+} and Fe^{3+} can lead to an enhancement in the CO oxidation rate over $\text{Pt-Fe}/\text{Al}_2\text{O}_3$ catalysts [48]. To probe the relevance of a redox cycle in the hydrogenation of carbonyl groups, we conducted an acetone hydrogenation control experiment with a $\text{Pt}/\text{H-ZSM-5}$ catalyst, which does not contain redox sites. The TOF of the $\text{Pt}/\text{H-ZSM-5}$ catalyst (69 min^{-1}) for acetone hydrogenation is similar to that of $\text{Pt}_1\text{Fe}_{0.2}/\text{SiO}_2$, suggesting that a redox cycle is not the dominant enhancement mechanism for hydrogenation of carbonyl groups. In addition, the similar turnover frequencies for $\text{Pt}_1\text{Fe}_x\text{O}_y$ and Pt_1Mo_x sites, where Mo is present in a more oxidized state compared to Fe as reported previously [49], further supports the absence of a redox cycle for carbonyl group hydrogenation. A 0.23 wt% Pt/SiO_2 catalyst, which

has similar dispersion to $\text{Pt}/\text{H-ZSM-5}$ as shown in Table S3, was prepared and studied to investigate the effect of the Pt particle size on the catalytic activity for acetone hydrogenation. The turnover frequency of 0.23 wt% Pt/SiO_2 is 5 min^{-1} , whereas the turnover frequencies for the two Pt/SiO_2 catalysts are much lower than $\text{Pt}/\text{H-ZSM-5}$, $\text{PtFe}_x\text{O}_y/\text{SiO}_2$ and $\text{PtMo}_x/\text{SiO}_2$. Thus, we suggest that the primary origin for enhanced activity is the formation of interfacial sites that increases the interaction of the $\text{C}=\text{O}$ bond with the catalyst surface.

4. Conclusions

The addition of Fe and Mo to Pt/SiO_2 catalysts increases the catalytic activity for the hydrogenation of carbonyl groups due to the formation of active sites at $\text{Pt-Fe}_x\text{O}_y$ and Pt-Mo_x interfaces. The catalytic activities of $\text{Pt-Fe}_x\text{O}_y$ ($r_{\text{PtFe}_x\text{O}_y}$) and Pt-Mo_x (r_{PtMo_x}) interfacial sites for acetone hydrogenation at 353 K and atmospheric pressure are 93 min^{-1} and 76 min^{-1} , respectively, indicating that the rates per $\text{Pt-Fe}_x\text{O}_y$ site ($r_{\text{PtFe}_x\text{O}_y}$) and Pt-Mo_x site (r_{PtMo_x}) are approximately 100 and 82 times greater, respectively, than that of the Pt site (r_{Pt}) for acetone hydrogenation to IPA. The catalytic activities of $\text{Pt-Fe}_x\text{O}_y$ ($r_{\text{PtFe}_x\text{O}_y}$) and Pt-Mo_x (r_{PtMo_x}) interfacial sites for 2-HY-THP hydrogenation at 393 K and 30 bar pressure are 480 min^{-1} and 830 min^{-1} , respectively, indicating that the rates per $\text{Pt-Fe}_x\text{O}_y$ site ($r_{\text{PtFe}_x\text{O}_y}$) and Pt-Mo_x site (r_{PtMo_x}) are approximately 60 and 100 times greater, respectively, than that of the Pt site (r_{Pt}) for 2-HY-THP hydrogenation to 1,5-PD. The

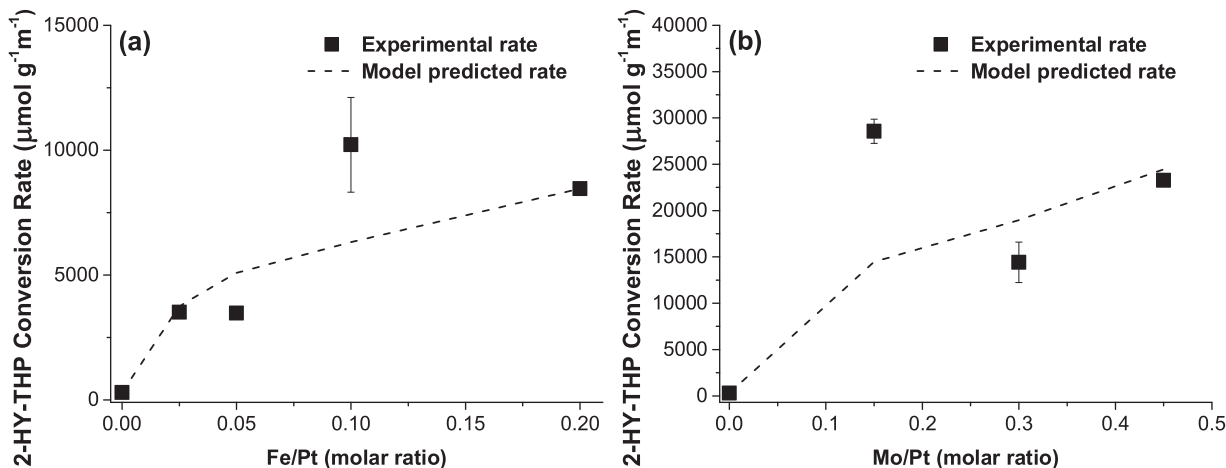


Fig. 7. Rate of 2-HY-THP hydrogenation over (a) $\text{Pt}_1\text{Fe}_x/\text{SiO}_2$ and (b) $\text{Pt}_1\text{Mo}_x/\text{SiO}_2$ catalysts. The dashed line indicates model predicted rates. The model predictions are as follows: $r_{\text{Pt}} = 7.8 \text{ min}^{-1}$, $r_{\text{PtFe}_x\text{O}_y} = 480 \text{ min}^{-1}$, and $r_{\text{PtMo}_x} = 830 \text{ min}^{-1}$.

formation of Pt- Fe_xO_y and Pt- MoO_x interfacial sites may help to stabilize reaction precursors and intermediates through interaction with $\text{C}=\text{O}$ moieties and thereby increase the rates of carbonyl hydrogenation reactions. The CSR methodology employed in this paper can be extended to other metal–metal oxide systems to understand the nature of the active sites for other reactions.

Acknowledgements

This material is based upon work supported by the Office of Basic Energy Sciences (DE-SC0014058). Partial support was also provided by the Department of Energy, Office of Energy Efficiency and Renewable Energy (DE-EE0006878). Use of facilities supported by the Wisconsin Materials Research Science and Engineering Center is also acknowledged (DMR-1121288). The authors acknowledge Dr. Canan Sener for the preparation of $\text{Pt}_1\text{Mo}_x/\text{SiO}_2$ catalysts and Samuel P. Burt for his help in *in situ* XPS analysis. I.B.A. acknowledges São Paulo Research Foundation (FAPESP, 2014/21988-7 and 2015/20477-1) for financial support. DZ acknowledges CNPq (National Counsel of Technological and Scientific Development) for financial support (309373/2014-0).

Appendix A. Supplementary data

Supplementary material related to this article can be found, in the online version, at doi:<https://doi.org/10.1016/j.apcatb.2018.02.058>.

References

- R. Alcalá, J. Greeley, M. Mavrikakis, J.A. Dumesic, Density-functional theory studies of acetone and propanal hydrogenation on Pt(111), *J. Chem. Phys.* 116 (2002) 8973–8980.
- M.A. Vannice, The influence of MSI (metal–support interactions) on activity and selectivity in the hydrogenation of aldehydes and ketones, *Top. Catal.* 4 (1997) 241–248.
- G.M.R. van Druten, L. Aksu, V. Ponec, On the promotion effects in the hydrogenation of acetone and propanal, *Appl. Catal. A* 149 (1997) 181–187.
- L.J. Durindell, C.M.A. Parlett, N.S. Hondonow, M.A. Isaacs, K. Wilson, A.F. Lee, Selectivity control in Pt-catalyzed cinnamaldehyde hydrogenation, *Sci. Rep.* 5 (2015).
- H. Wang, J.M. Krier, Z. Zhu, G. Melaet, Y. Wang, G. Kennedy, S. Alayoglu, K. An, G.A. Somorjai, Promotion of hydrogenation of organic molecules by incorporating iron into platinum nanoparticle catalysts: displacement of inactive reaction intermediates, *ACS Catal.* 3 (2013) 2371–2375.
- H.G. Manyar, C. Paun, R. Pilus, D.W. Rooney, J.M. Thompson, C. Hardacre, Highly selective and efficient hydrogenation of carboxylic acids to alcohols using titania supported Pt catalysts, *Chem. Commun.* 46 (2010) 6279–6281.
- M. Englisch, V.S. Ranade, J.A. Lercher, Hydrogenation of crotonaldehyde over Pt based bimetallic catalysts, *J. Mol. Catal. A Chem.* 121 (1997) 69–80.
- J. Lee, Y.T. Kim, G.W. Huber, Aqueous-phase hydrogenation and hydro-deoxygenation of biomass-derived oxygenates with bimetallic catalysts, *Green Chem.* 16 (2014) 708–718.
- A. Siani, O.S. Alexeev, G. Lafaye, M.D. Amiridis, The effect of Fe on SiO_2 -supported Pt catalysts: structure, chemisorptive, and catalytic properties, *J. Catal.* 266 (2009) 26–38.
- J.R. Kitchin, J.K. Nørskov, M.A. Bartaeu, J.G. Chen, Role of strain and ligand effects in the modification of the electronic and chemical properties of bimetallic surfaces, *Phys. Rev. Lett.* 93 (2004) 156801.
- J.R. Kitchin, J.K. Nørskov, M.A. Bartaeu, J.G. Chen, Modification of the surface electronic and chemical properties of Pt(111) by subsurface 3d transition metals, *J. Chem. Phys.* 120 (2004) 10240–10246.
- K. Balakrishnan, J. Schwank, Neopentane reactions over bimetallic Pt-Sn/ Al_2O_3 and Pt-Au/ SiO_2 catalysts, *J. Catal.* 132 (1991) 451–464.
- D. Richard, J. Ockelford, A. Giroir-Fendler, P. Gallezot, Composition and catalytic properties in cinnamaldehyde hydrogenation of charcoal-supported, platinum catalysts modified by FeCl_2 additives, *Catal. Lett.* 3 (1989) 53–58.
- Z.J. Brentzel, K.J. Barnett, K. Huang, C.T. Maravelias, J.A. Dumesic, G.W. Huber, Chemicals from biomass: combining ring-opening tautomerization and hydrogenation reactions to produce 1,5-pentanediol from furfural, *ChemSusChem* 10 (2017) 1351–1355.
- I. Ro, R. Carrasquillo-Flores, J.A. Dumesic, G.W. Huber, Intrinsic kinetics of plasmon-enhanced reverse water gas shift on Au and Au–Mo interfacial sites supported on silica, *Appl. Catal. A* 521 (2016) 182–189.
- I. Ro, Y. Liu, M.R. Ball, D.H.K. Jackson, J.P. Chada, C. Sener, T.F. Kuech, R.J. Madon, G.W. Huber, J.A. Dumesic, Role of the Cu-ZrO₂ interfacial sites for conversion of ethanol to ethyl acetate and synthesis of methanol from CO₂ and H₂, *ACS Catal.* 6 (2016) 7040–7050.
- I. Ro, C. Sener, T.M. Stadelman, M.R. Ball, J.M. Venegas, S.P. Burt, I. Hermans, J.A. Dumesic, G.W. Huber, Measurement of intrinsic catalytic activity of Pt monometallic and Pt-MoO_x interfacial sites over visible light enhanced PtMoO_x/SiO₂ catalyst in reverse water gas shift reaction, *J. Catal.* 344 (2016) 784–794.
- R. Carrasquillo-Flores, I. Ro, M.D. Kumbhalkar, S. Burt, C.A. Carrero, A.C. Alba-Rubio, J.T. Miller, I. Hermans, G.W. Huber, J.A. Dumesic, Reverse water–gas shift on interfacial sites formed by deposition of oxidized molybdenum moieties onto gold nanoparticles, *J. Am. Chem. Soc.* 137 (2015) 10317–10325.
- I. Ro, I.B. Aragao, J.P. Chada, Y. Liu, K.R. Rivera-Dones, M.R. Ball, D. Zanchet, J.A. Dumesic, G.W. Huber, The role of Pt- Fe_xO_y interfacial sites for CO oxidation, *J. Catal.* 358 (2018) 19–26.
- I.B. Aragao, I. Ro, Y. Liu, M. Ball, G.W. Huber, D. Zanchet, J.A. Dumesic, Catalysts synthesized by selective deposition of Fe onto Pt for the water–gas shift reaction, *Appl. Catal. B: Environ.* 222 (2018) 182–190.
- Y. Liu, F. Göeltl, I. Ro, M.R. Ball, C. Sener, I.B. Aragão, D. Zanchet, G.W. Huber, M. Mavrikakis, J.A. Dumesic, Synthesis gas conversion over Rh-based catalysts promoted by Fe and Mn, *ACS Catal.* 7 (2017) 4550–4563.
- J. Kim, W. Kim, Y. Seo, J.-C. Kim, R. Ryoo, *n*-heptane hydroisomerization over Pt/MFI zeolite nanosheets: effects of zeolite crystal thickness and platinum location, *J. Catal.* 301 (2013) 187–197.
- J.Y. Shen, J.M. Hill, R.M. Watwe, B.E. Spiewak, J.A. Dumesic, Microcalorimetric, infrared spectroscopic, and DFT studies of ethylene adsorption on Pt/SiO₂(2) and Pt-Sn/SiO₂(2) catalysts, *J. Phys. Chem. B* 103 (1999) 3923–3934.
- B.J. O'Neill, D.H.K. Jackson, A.J. Crisci, C.A. Farberow, F. Shi, A.C. Alba-Rubio, J. Lu, P.J. Dietrich, X. Gu, C.L. Marshall, P.C. Stair, J.W. Elam, J.T. Miller, F.H. Ribeiro, P.M. Voyles, J. Greeley, M. Mavrikakis, S.L. Scott, T.F. Kuech, J.A. Dumesic, Stabilization of copper catalysts for liquid-phase reactions by atomic layer deposition, *Angew. Chem. Int. Ed.* 52 (2013) 13808–13812.
- S.H. Hakim, C. Sener, A.C. Alba-Rubio, T.M. Gostanian, B.J. O'Neill, F.H. Ribeiro, J.T. Miller, J.A. Dumesic, Synthesis of supported bimetallic nanoparticles with controlled size and composition distributions for active site elucidation, *J. Catal.* 328 (2015) 75–90.
- I.B. Aragao, I. Ro, Y. Liu, M.R. Ball, G.W. Huber, D. Zanchet, J.A. Dumesic, Catalysts synthesized by selective deposition of Fe onto Pt for the water–gas shift reaction, *Appl. Catal. B: Environ.* 222 (2018) 182–190, <http://dx.doi.org/10.1016/j.apcatb.2017.10.004> FYI.
- S. Ikeda, S. Ishino, T. Harada, N. Okamoto, T. Sakata, H. Mori, S. Kuwabata, T. Torimoto, M. Matsumura, Ligand-free platinum nanoparticles encapsulated in a hollow porous carbon shell as a highly active heterogeneous hydrogenation catalyst, *Angew. Chem. Int. Ed.* 45 (2006) 7063–7066.
- M. Alnot, V. Gorodetskii, A. Cassuto, J.J. Ehrhardt, Auger electron spectroscopy, X-ray photoelectron spectroscopy, work function measurements and photoemission of adsorbed xenon on thin films of Pt-Re(111) alloys, *Thin Solid Films* 151 (1987) 251–262.
- P. Kannan, T. Maiyalagan, N.G. Sahoo, M. Opallo, Nitrogen doped graphene nanosheet supported platinum nanoparticles as high performance electrochemical homocysteine biosensors, *J. Mater. Chem. B* 1 (2013) 4655–4666.
- B. Qiao, A. Wang, X. Yang, L.F. Allard, Z. Jiang, Y. Cui, J. Liu, J. Li, T. Zhang, Single-atom catalysis of CO oxidation using Pt1/FeOx, *Nat. Chem.* 3 (2011) 634–641.
- S. Gota, E. Guiot, M. Henriot, M. Gautier-Soyer, Atomic-oxygen-assisted MBE growth of alpha-Fe₂O₃ on alpha-Al₂O₃(0001): metastable FeO(111)-like phase at subnanometer thicknesses, *Phys. Rev. B* 60 (1999) 14387–14395.
- Y. Tang, Y. Shao, N. Chen, X. Liu, S.Q. Chen, K.F. Yao, Insight into the high reactivity of commercial Fe-Si-B amorphous zero-valent iron in degrading azo dye solutions, *RSC Adv.* 5 (2015) 34032–34039.
- M. Preisinger, M. Krispin, T. Rudolf, S. Horn, D.R. Strongin, Electronic structure of nanoscale iron oxide particles measured by scanning tunneling and photoelectron spectroscopies, *Phys. Rev. B* 71 (2005).
- H. Yoshida, N. Igarashi, S.-i. Fujita, J. Panpranot, M. Arai, Influence of crystallite size of TiO₂ supports on the activity of dispersed Pt catalysts in liquid-phase selective hydrogenation of 3-nitrostyrene, nitrobenzene, and styrene, *Catal. Lett.* 145 (2015) 606–611.
- H. Yoshida, S. Narisawa, S.-i. Fujita, L. Ruixia, M. Arai, In situ FTIR study on the formation and adsorption of CO on alumina-supported noble metal catalysts from H₂ and CO₂ in the presence of water vapor at high pressures, *Phys. Chem. Chem. Phys.* 14 (2012) 4724–4733.
- F. Bocuzzi, A. Chiorino, E. Guglielminotti, Effects of structural defects and alloying on the FTIR spectra of CO adsorbed on PtZnO, *Surf. Sci.* 368 (1996) 264–269.
- R.K. Brandt, M.R. Hughes, L.P. Bourget, K. Truszkowska, R.G. Greenler, The interpretation of CO adsorbed on Pt/SiO₂ of two different particle-size distributions, *Surf. Sci.* 286 (1993) 15–25.
- R.K. Brandt, R.S. Sorbello, R.G. Greenler, Site-specific, coupled-harmonic-oscillator model of carbon monoxide adsorbed on extended, single-crystal surfaces and on small crystals of platinum, *Surf. Sci.* 271 (1992) 605–615.
- K. Balakrishnan, A. Sachdev, J. Schwank, Chemisorption and FTIR study of bimetallic Pt-Au/SiO₂ catalysts, *J. Catal.* 121 (1990) 441–455.
- K. Ding, A. Gulec, A.M. Johnson, N.M. Schweitzer, G.D. Stucky, L.D. Marks, P.C. Stair, Identification of active sites in CO oxidation and water–gas shift over supported Pt catalysts, *Science* 350 (2015) 189–192.
- A.D. Allian, K. Takabane, K.L. Fujdala, X. Hao, T.J. Truex, J. Cai, C. Buda, M. Neurock, E. Iglesia, Chemisorption of CO and mechanism of CO oxidation on supported platinum nanoclusters, *J. Am. Chem. Soc.* 133 (2011) 4498–4517.
- J.Z. Xu, J.T. Yates, Terrace width effect on adsorbate vibrational comparison of pt(335) and pt(112) for chemisorption of CO, *Surf. Sci.* 327 (1995) 193–201.
- B. Sen, M.A. Vannice, Metal–support effects on acetone hydrogenation over platinum catalysts, *J. Catal.* 113 (1988) 52–71.
- R. Hirsch, F. Delbecq, P. Sautet, J. Hafner, Adsorption of unsaturated aldehydes on

the (111) surface of a Pt–Fe alloy catalyst from first principles, *J. Catal.* 217 (2003) 354–366.

[45] R.D. Cortright, J.M. Hill, J.A. Dumesic, Selective dehydrogenation of isobutane over supported Pt/Sn catalysts, *Catal. Today* 55 (2000) 213–223.

[46] R.D. Cortright, P.E. Levin, J.A. Dumesic, Kinetic studies of isobutane dehydrogenation and isobutene hydrogenation over Pt/Sn-based catalysts, *Ind. Eng. Chem. Res.* 37 (1998) 1717–1723.

[47] C.M. Kalamaras, P. Panagiotopoulou, D.I. Kondarides, A.M. Efstathiou, Kinetic and mechanistic studies of the water–gas shift reaction on Pt/TiO₂ catalyst, *J. Catal.* 264 (2009) 117–129.

[48] A. Tomita, K.-i. Shimizu, K. Kato, T. Akita, Y. Tai, Mechanism of low-temperature CO oxidation on Pt/Fe-containing alumina catalysts pretreated with water, *J. Phys. Chem. C* 117 (2013) 1268–1277.

[49] C. Sener, T.S. Wesley, A.C. Alba-Rubio, M.D. Kumbhalkar, S.H. Hakim, F.H. Ribeiro, J.T. Miller, J.A. Dumesic, PtMo bimetallic catalysts synthesized by controlled surface reactions for water gas shift, *ACS Catal.* 6 (2016) 1334–1344.